ACS Energy LETTERS

http://pubs.acs.org/journal/aelccp

LETTER

Plasma Activated Electrochemical Ammonia Synthesis from Nitrogen and Water

Rakesh K. Sharma,* Hrishikesh Patel, Usman Mushtaq, Vasileios Kyriakou, Georgios Zafeiropoulos, Floran Peeters, Stefan Welzel, Mauritius C. M. van de Sanden, and Mihalis N. Tsampas*

Cite This: *ACS Energy Lett.* 2021, 6, 313−319

Read Online

ACCESS | Metrics & More | Article Recommendations | Supporting Information

ABSTRACT: **Ammonia is an important precursor of fertilizers, as well as a potential carbon-free energy carrier. Nowadays, ammonia is synthesized via the Haber−Bosch process, which is a capital- and energy-intensive process with an immense CO_2 footprint. Thus, alternative processes for the sustainable and decentralized ammonia production from N_2 and H_2O using renewable electricity are required. The key challenges for the realization of such processes are the efficient activation of the N_2 bond and selectivity toward NH_3. In this contribution, we report an all-electric method for sustainable ammonia production from nitrogen and water using a plasma-activated proton conducting solid oxide electrolyzer. Hydrogen species produced by water oxidation over the anode are transported through the proton conducting membrane to the cathode where they react with the plasma-activated nitrogen toward ammonia. Ammonia production rates and Faradaic efficiencies up to of 26.8 nmol of NH_3 s^{-1} cm^{-2} and 88%, respectively, were achieved.**

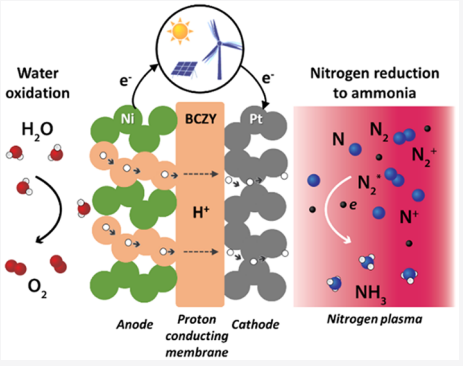

Ammonia, from which virtually all nitrogen-containing compounds are derived, is a major and valuable raw material for industry and agriculture.[1,2] In fact, the fertilizers generated from the ammonia such as ammonium nitrates, phosphates, and urea are responsible for sustaining one-third of the Earth's population.[3] Moreover, 1 mol of ammonia contains 17.6 wt % of hydrogen (108 g H_2/L) at 20 °C, which is highly desirable for the transportation[4] as well as for storing intermittent renewable energy such as wind and solar.[5,6] In addition, ammonia has been intensively studied for its potential use as sustainable fuel source[7,8] and other off-grid power applications.[9]

Nitrogen-based fertilizer demand is growing rapidly and estimated to show a two or three-folded increase in the second half of the 21st century.[10] To date, approximately 500 million tonnes of ammonia are produced per year via the Haber−Bosch (H−B) process, accounting for 3−5% of total natural gas consumption worldwide and 2% of global energy usage.[2,10] H−B requires a large fossil fuel energy input, high temperatures (400−600 °C) and pressures (200−400 atm) as well as a significant capital investment.[11−15] These intense conditions are the main disadvantages of the H−B process, as they prevent the possibility of lowering capital costs,[16] decentralization, and small-scale ammonia production at the level of local communities. Moreover, the world's hydrogen, which is also a key reactant in ammonia production, is produced primarily from the steam re-forming of methane, emitting huge amounts of CO_2 that account for 1.6% of global emissions per year.[2,15] Therefore, alternative technologies need to be explored for ammonia synthesis, which occur under more moderate conditions,[17] require less carbon input,[18] or can be powered by intermittent renewable energy sources.[19]

Nowadays, plasma technology has attracted a lot of attention as an alternative method of clean ammonia synthesis, including a renewable pathway that coupled this technology with other renewable energy approaches. At low temperature, plasmas are reported as one of the most efficient approaches for rupturing the triple nitrogen bond,[20−24] which is the fundamental requirement for the ammonia synthesis. Most of the studies on plasma-assisted ammonia synthesis are based on atmospheric pressure dielectric barrier discharge plasma over various catalytic systems, with nitrogen conversion between 0.2 and 7.8% in N_2/H_2 mixtures.[25−30] There are also approaches in which plasma activation of nitrogen and water vapor (as a hydrogen source) have been investigated for ammonia synthesis offering promising results in terms of selectivity.[31−34] However, there are a few studies on the synthesis of ammonia from nitrogen−

Received: November 7, 2020
Accepted: December 14, 2020
Published: December 31, 2020

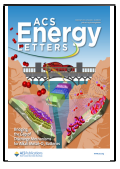

https://dx.doi.org/10.1021/acsenergylett.0c02349
ACS Energy Lett. 2021, 6, 313−319

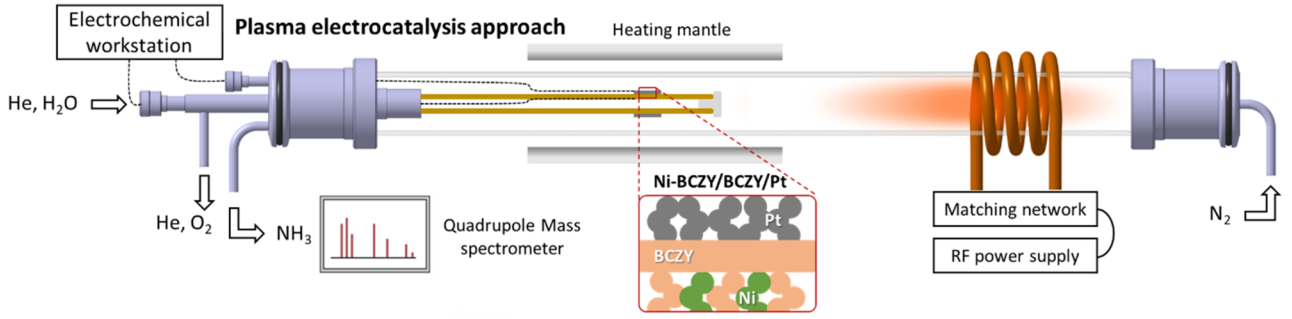

Figure 1. Schematic representation of hybrid plasma electrochemical reactor setup.

hydrogen using low-pressure (0.01−10 Torr) discharges.[35−40] In fact, low-pressure nitrogen discharges are well-known for efficiently producing vibrationally excited molecules that can further generate atomic nitrogen via a vibrational dissociation channel.[41−44] Despite the potential benefits of plasma technologies, such as localized and environmentally friendly energy storage through chemical conversion, the two most critical challenges for upscaling this technology are the efficient dinitrogen fixation and suppression of the reverse reactions. Hence, suitable catalysts with stronger plasma synergistic activities and optimized reactor designs are required to overcome these challenges.[45,46]

Electrochemical processes for ammonia synthesis have also gathered enormous interest since one can synthesize ammonia directly from water and nitrogen in a single device, thus decreasing the complexity and carbon footprint of the conventional Haber−Bosch process.[47−57] However, the upscaling of this technology is primarily hindered by low rates and/or selectivity (Faradaic efficiency) due to the challenge of dinitrogen triple bond cleavage at a rate that is comparable to the hydrogen evolution reaction rate. Recent efforts are directed in the development of more efficient electrode materials or modification of the electrode environment to suppress HER and thus improving Faradaic efficiency (FE) toward ammonia synthesis.[55,56] The best reported performance in liquid and solid electrolyte electrochemical cells are ∼66% FE at 6.36 mA/cm^2 (14.5 nmol s^{-1} cm^{-2}) and ∼78% FE at 1.15 mA/cm^2 (5.6 nmol s^{-1} cm^{-2}) respectively.[55,57]

The combination of N_2 plasma with electrochemical cells has been recently proposed as an alternative way for nitrogen fixation.[24,58,59] In these systems plasma is utilized for nitrogen activation and electrochemical cells for providing the coreactants. Hawtof et al.[58] have reported a hybrid approach where the electrical circuit of the plasma is integrated with the electrolysis one, allowing ammonia synthesis in the absence of nitrogen reduction electrode. The FE of this approach has reached values of up to ∼100% at 2.5 mA (8.63 nmol/s, the rate is not normalized per surface area due to the electrodeless configuration).[58] Kumari et al.[59] have reported a polymer electrolyte membrane plasma integrated system, where plasma activation leads up to 47% increase on the ammonia production vs pure electrochemical approach. Due to poor Faradaic efficiency the ammonia formation rate was 0.05 nmol s^{-1} cm^{-2}.[59]

Inspired by the promising plasma electrochemical integrated systems, we have developed a plasma activated proton conducting solid oxide electrolysis cell (H-SOEC), as shown in Figure 1. At the anode, water oxidation (at the anode: $H_2O(g) \rightarrow 2H^+ + {}^1/_2O_2(g) + 2e^-$) takes place, which produces protons (H^+). These protons are transported to the cathode via proton conducting membrane where they either form molecular hydrogen or react with the activated nitrogen and form the NH_3. In this approach, both the reactions (water oxidation and nitrogen reduction to ammonia) are taking place in two different compartments, thus allowing two independent knobs of operation. To further understand the potential of the plasma aided electrochemical approach, we have benchmarked this pathway with the classical pure plasma (without the presence of catalyst) and plasma-assisted catalysis (where both the reactants H_2 and N_2 are coinjected and coactivated).

Figure 1 shows the schematic of our in-house built reactor to test the N_2 plasma-assisted proton conducting solid oxide (H-SOEC) electrolyzer. H-SOEC is based on commercial half-anode supported cell Ni-BCZY/BCZY (where BCZY is the abbreviation of $BaCe_{0.2}Zr_{0.7}Y_{0.1}O_{3-\delta}$) and a Pt cathode. The microstructure of the Pt catalyst is porous and consists of a network of percolated particles of the order of a micron (Figure S1). Such a porous microstructure is desired for efficient diffusion of the reactant gases and for creating a high surface area (interfacial area of particle and pore) as well as a triple phase boundary (TBP: electrolyte−electrode−gases).

To determine the role of electrochemical and plasma-assisted electrochemical ammonia synthesis, a transient experiment was carried out at 500 °C by sequentially varying the applied current (from 0 to 5 mA) and the plasma power (from 0 to 80 W), as shown in Figure 2. The reactions on each electrode are mentioned below with and without plasma activation.

Anode:

$$H_2O(g) \rightarrow 2H^+(BCZY) + \frac{1}{2}O_2(g) + 2e^- \quad (1)$$

Cathode:

$$2H^+(BCZY) + 2e^- \rightarrow H_2(g) \quad (2)$$

$$6H^+(BCZY) + N_2(g) + 6e^- \rightarrow 2NH_3(g) \quad (3)$$

Plasma ON:

$$3xH^+(BCZY) + N_x(g) + 3xe^- \rightarrow xNH_3(g) \quad (4)$$

The rate of NH_3 formation under open-circuit ($I = 0$) and plasma off conditions is zero due to the absence of the hydrogen species on the cathode. Upon applying current (i.e., galvanostatic mode) of 5 mA (at $t = 20$ min), protons (H^+) from water oxidation (eq 1) reach the cathode (via the membrane), forming molecular hydrogen of ∼5.14 nmol of H_2 s^{-1} cm^{-2} from their associative desorption (eq 2). In the absence

https://dx.doi.org/10.1021/acsenergylett.0c02349
ACS Energy Lett. 2021, 6, 313−319

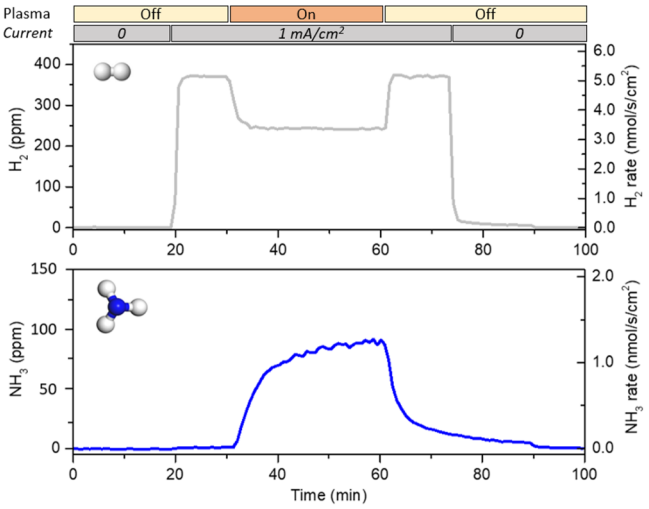

Figure 2. H_2 and NH_3 production rate 500 °C upon sequential step changes of the applied current (5 mA) and plasma (80 W), respectively.

of nitrogen plasma activation, no ammonia concentration was detected and this can be attributed to the low operating pressure and the poor electrochemical nitrogen reduction (eq 3) activity of Pt.[60] Upon plasma ignition (at t = 30 min) in the presence of the same applied current, NH_3 formation starts taking place (eq 4) with a simultaneous decrease of the hydrogen evolution and a steady state is reached after ∼4 min. Rate of NH_3 production (1.21 nmol of NH_3 s^{-1} cm^{-2}) is roughly two-thirds the rate of hydrogen consumption (1.80 nmol of H_2 s^{-1} cm^{-2}), which is consistent with reaction stoichiometry. The corresponding conversion of nitrogen to ammonia is 0.045% at 1 mA/cm^2. Once plasma is switched off at t = 60 min, the NH_3 production rate gradually returns to zero, while hydrogen formation returns to its initial value and, on further interrupting the current at t = 73 min, both NH_3 and hydrogen signals drop to zero.

Figure 3a shows the current vs voltage (I−V) curves of proton conducting electrolyzer at 500 °C. Under steady-state conditions no electrolysis current is observed, irrespective of plasma conditions (on or off), as expected. The electrolysis current (current density) steadily increased with the applied

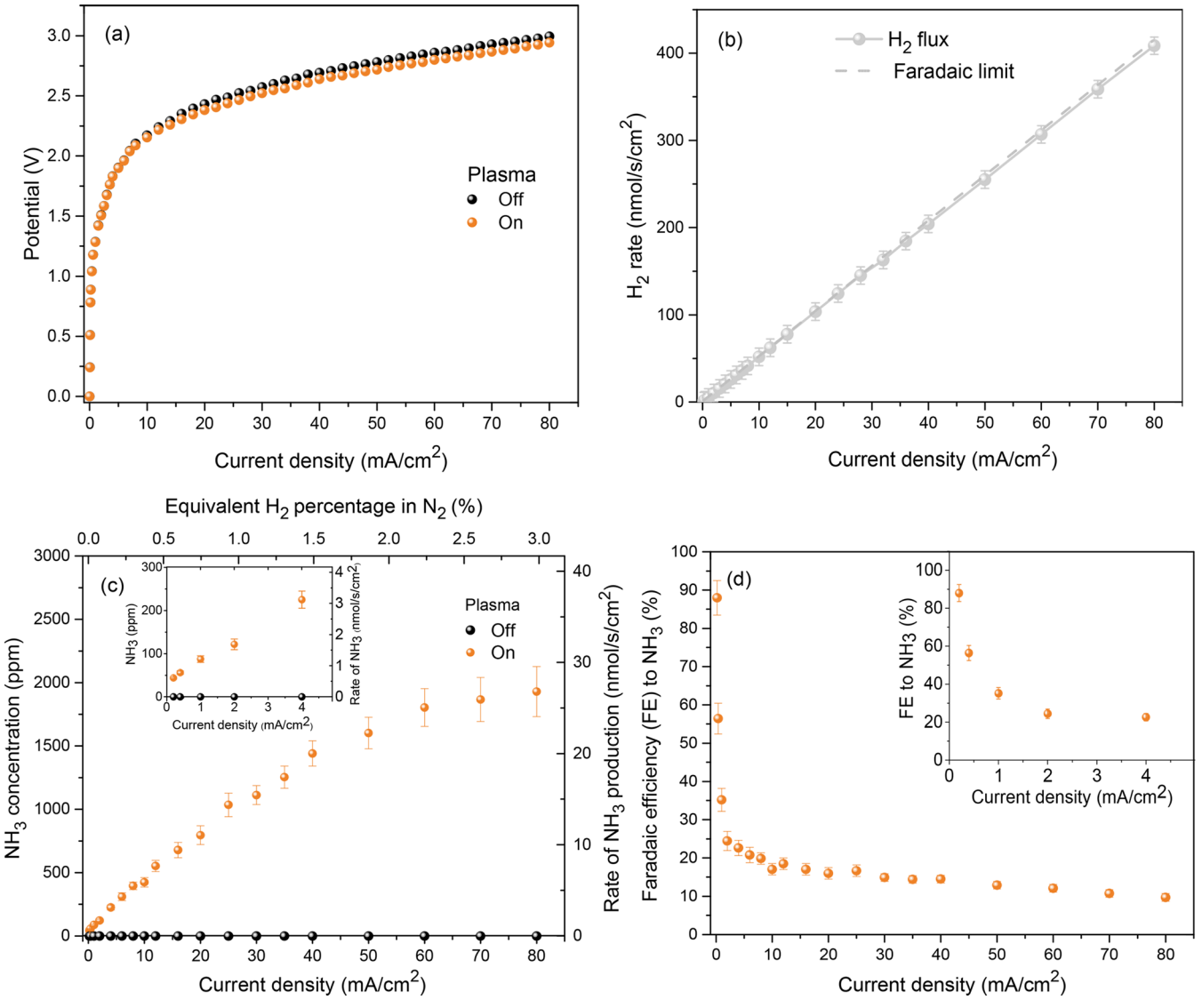

Figure 3. I−V characteristics (a), effect of current on the rate of H_2 (b) and NH_3 (c) production, and Faradaic efficiency of NH_3 production (d) at 500 °C and 80 W plasma power.

https://dx.doi.org/10.1021/acsenergylett.0c02349
ACS Energy Lett. 2021, 6, 313−319

voltage beyond 1.2 V, which leads to H_2 production at the cathode, as shown Figure 3b. With increasing current, H_2 production increases as expected. The $I-V$ curves with and without plasma are almost identical. This observation was also verified by the electrochemical impedance spectra (Figure S2) in which the polarization resistance practically remained the same. Therefore, plasma activation does not seem to interfere significantly with charge transfer on the cathode. Moreover, there is no plasma heating impact on the plasma electrode since it is far (i.e., 10−15 cm, defined as plasma afterglow) from the tail of the active plasma zone, as demonstrated in our previous work. Thus, plasma activation does not have any short-term detrimental effects on the functioning of the electrolyzer.

Parts c and d of Figure 3 show the rate of NH_3 formation and corresponding Faradaic efficiency (i.e., selectivity to ammonia formation) under bias with plasma conditions (80 W) as a function of applied current. Upon current application, protons arriving on the Pt/BCZY interface are diffused on the catalyst surface as adsorbates, where they can either react with activated nitrogen species for NH_3 formation (eq 3) or with coadsorbed proton species for the formation of molecular hydrogen (eq 2).

In the low-current range, production of NH_3 increases with the applied current since in this current range, reaction is limited by the supply of hydrogen species (Figure 3c), whereas at higher current densities, NH_3 production keeps increasing but with lower rate. Due to the architecture of our electrode (i.e., porous electronic conducting film with 10 μm thickness deposited on proton conducting support), the reaction zone is extended as the applied current (flux of protons) is increased.[61] At low current densities, protons are diffused as adsorbates on the vicinity of the triple phase boundaries (TPB), i.e., the electrode (Pt), electrolyte (BSZY), and gas (activated nitrogen) interface, whereas at high current densities the hydrogen species are diffused to areas further away from the TPB and thus the ammonia production keeps increasing. Faradaic efficiency decreases from 88% at 0.2 mA/cm^2 to 10% at 80 mA/cm^2 with increasing current (Figure 3d), suggesting that the vicinity of the TPB is more active for nitrogen fixation when compared to the rest of electrode.

Another important metric in catalytic studies which is not usually reported, is the turnover frequency (TOF), which quantifies the specific activity of a catalytic center by the number of catalytic cycles occurring at the center per unit time. It is usually difficult to define TOF for plasma studies since the quantification of plasma interaction with the reactor walls and/or catalyst is not straightforward. However, in our approach due to the separation of the reactants (via the proton conducting membrane), the reaction zone is limited to catalyst surface, which simplifies the estimation of TOF.

In addition the use of Pt as cathode has the advantage to offer a reliable way to define the electrochemical active surface area (ECSA). ECSA of Pt can be defined by the well-established method of hydrogen under potential deposition (HUPD).[62] ECSA of Pt electrode, estimated from HUPD (Figure S3), is equal to 10.5 nmol of Pt per nominal electrode cm^2. This allows us to estimate the TOF, which is depicted as a function of current density in Figure S4. As one can see, a value of ∼2.6 s^{-1} is obtained, which is quite high when compared with the ∼0.1 s^{-1} of the Haber−Bosch process.[63]

The effect of plasma power, which may affect the distribution of excited states and their flux to the electrocatalyst surface, has also been studied. By estimating the plasma volume from the photographs in Figure S5, it is observed that the plasma volume increases linearly with power. As shown in the Supporting Information, the power density remains constant at approximately 0.6 W/cm^3 in all cases, leading to similar plasma properties for all plasma powers. Therefore, it can be concluded that the largest difference in conditions between different plasma powers comes from the growth of the plasma volume and the corresponding reduction of the distance between the plasma edge and the electrolyzer surface. As discussed in the Supporting Information, plasma conditions are very similar to those modeled in the work of Guerra et al., who include the development of plasma-activated species downstream of the nitrogen plasma.[64] Assuming a constant axial gas flow velocity between the plasma edge and catalyst surface, a time-of-flight for plasma-activated species of ∼200 ms at 40 W to ∼100 ms at 120 W has been estimated from the photographs in Figure S5. Comparing with the N_2 plasma model by Guerra et al., both vibrationally excited N_2 and atomic N can reach the electrode at significant concentrations. Particularly, highly energetic $N_2(\nu > 10)$ can impinge on the electrolyzer at mole fractions of $>10^{-4}$, and atomic nitrogen at mole fractions $>10^{-3}$ and even with higher mole fractions as the plasma edge moves closer to the electrolyzer surface.[64] The increase in ammonia formation rates with increasing plasma power can, therefore, be assigned to an increasing flux of one or both of these energetic nitrogen species to the electrolyzer. As discussed in the Supporting Information, the poorer performance at 120 W compared to 80 W could be due to a decreased flux of $N_2(\nu > 10)$ to the electrolyzer surface, but experimental quantification of the fluxes of energetic nitrogen species will be required before definitive conclusions can be drawn.

Furthermore, pure plasma (without SOEC) and plasma-assisted catalysis (with SOEC but at open circuit conditions) have been carried out at 500 °C, where the reactants (H_2 and N_2) were coactivated by RF-plasma, as shown schematically in Figure S6. From Figure 3c,d and Figure S6 (bottom), it is clear that the plasma-assisted electrochemical approach (1930 ppm of NH_3, 10% H_2 conversion) is better than either pure plasma (990 ppm of NH_3, 5% H_2 conversion) or plasma-assisted catalysis (1185 ppm of NH_3, 6% H_2 conversion) in terms of rate and hydrogen conversion at 500 °C and 80 mA/cm^2 current density or equivalent hydrogen. This can be attributed to the different adsorption pathways for hydrogen species involved in each process, i.e., via the protonic conducting membrane and gas phases, respectively. However, direct comparison between pure plasma and plasma-assisted catalysis with electrocatalysis is not straightforward since addition of H_2 to the plasma will affect the densities of activated molecules. With the ionization potential (and electron impact ionization cross sections) being very similar for N_2 and H_2, the electron density and electron temperature will not change radically when adding H_2, but the $N_2(\nu)$ and N densities arriving at the catalytic surface may still decrease significantly simply from dilution by H_2.[20,21,65] Furthermore, it has been shown that in pure N_2 plasma up to 70% of electrical power is deposited as internal energy, and up to 35% specifically in vibrational modes, of the N_2 molecule.[43] The addition of H_2 will cause a significant fraction of the input power to go toward the internal energy of H_2 as well as into dissociation of H_2. Especially the latter will reduce N densities significantly as the H_2 content increases, since the lower dissociation energy of H_2 (4.5 eV) compared to N_2 (9.8 eV) will lead to preferential deposition of plasma power into H_2 dissociation.[66]

Thermodynamic calculations have been also carried out for the equilibrium concentration of NH_3 in the N_2, H_2, and NH_3

https://dx.doi.org/10.1021/acsenergylett.0c02349
ACS Energy Lett. 2021, 6, 313−319

mixture as a function of temperature and pressure for 3% H_2 in N_2 (Figure S7). The performance observed in our approach is ∼4 orders of magnitude higher than the thermodynamic equilibrium at the same temperature and pressure. To realize this difference, a conventional thermochemical reactor operating at thermodynamic equilibrium would require ∼100 bar pressure to produce the same amount of NH_3.

To benchmark the performance of our plasma-assisted electrochemical ammonia synthesis reactor with other studies for electrochemical ammonia synthesis (which is based on the similar reactor configuration but without the plasma activation), a comparison to literature for formation rates and Faradaic efficiencies to NH_3 has been also shown in Figure S8. Typical rate and Faradaic efficiencies in this work are higher than reported in the literature for proton conducting solid oxide electrolyzers. Overall, achieved ammonia production rates for the plasma-assisted electrochemical approach is in the range $(0.1-2.6) \times 10^{-8}$ mol s^{-1} cm^{-2} with Faradaic efficiency varying from 88 to 10%, which is 5 times lower than required to satisfy the commercial needs, i.e., rate = 10^{-7} mol s^{-1} cm^{-2} and Faradaic efficiency at least 50%.[47] We believe that these numbers can be achieved with appropriate reactor optimization. To extend our comparison to other electrochemically driven systems, we also mention the lithium-mediated approaches.[67,68] In such systems, a Faradaic efficiency up to 88.5% has been reported, which is similar to the efficiency obtained in this work. Nevertheless, the lithium-mediated approaches are multistep processes, whereas in our system the hydrogen production/purification and nitrogen fixation take place in a single step.

The energy consumption in our system for plasma-assisted electrochemical approach is 605 MJ/(N mol), which is within the range of reported values (95 to 2698 MJ/(N mol)) for N_2 fixation by H_2O.[31−33] However, the reactor in this work demonstrates a proof-of-concept for plasma-assisted electrochemical NH_3 synthesis with a very high formation rate and Faradaic conversion. A further reactor optimization is required in order to have more optimized energy consumption and NH_3 production. For instance, as mentioned above, the cross-sectional area of the plasma discharge in our setup is much higher than the cross-section/active area of cathode electrocatalyst, due to which most of the activated N_2 species bypass the electrocatalyst and hence do not contribute in the NH_3 synthesis. Moreover, a Pt cathode electrocatalyst has been used, which is highly active for HER kinetics.[47−49] Recent theoretical studies have suggested that a more selective catalyst for nitrogen reduction reaction or with lower hydrogen evolution activity, such as Co, Ni, and Ru, respectively, could significantly improve the NH_3 formation rate.[45,46] The effect of electrode microstructure on ammonia production is also essential since porosity, particle size, TPB length, and tortuosity play a key role on the accessibility of activated nitrogen and hydrogen species on the reactive sites. Correlation of the microstructural characteristic with ammonia production can only be realized with structured electrode.[69] In future work, these possibilities will be investigated experimentally and combined with plasma modeling for the particular reactor geometry under study here.

To summarize, we have demonstrated that plasma-activated nitrogen can be combined with electrochemically generated surface hydrogen species to achieve an alternative, all-electric nitrogen fixation pathway. The highest NH_3 production rate is 26.8 nmol s^{-1} cm^{-2}, corresponding to a TOF of 2.6 s^{-1} at 80 mA/cm^2 with a 10% Faradaic efficiency. Interestingly, at lower current density Faradaic efficiency up to 88% (with rate and TOF of 0.61 nmol s^{-1} cm^{-2} and 0.059 s^{-1} respectively) was achieved. This novel plasma-assisted electrochemical approach was benchmarked and proved superior to the individual pure plasma and plasma catalysis approaches, in which gas phase hydrogen is cofed and activated with nitrogen by the plasma source. We expect that performance can be further enhanced by improving the interaction of activated nitrogen species with electrocatalyst (via utilization of advanced SOEC architectures and reactor design) and adjusting the operational parameters of the plasma.

■ ASSOCIATED CONTENT

Supporting Information

The Supporting Information is available free of charge at https://pubs.acs.org/doi/10.1021/acsenergylett.0c02349.

Experimental details, microstructural characterization of the Ni-BCZY/BCZY/Pt cell, SEM images, Nyquist plot of Ni-BCZY/BCZY/Pt at OCV with and without plasma, CV, active surface area calculation, turn over frequency (TOF) calculation, effect of plasma power on NH_3 synthesis, pure plasma and plasma catalysis approaches, equilibrium concentration of ammonia, and benchmarking our approach with electrochemical ammonia synthesis: present study vs literature (PDF)

■ AUTHOR INFORMATION

Corresponding Authors

Rakesh K. Sharma − *Dutch Institute for Fundamental Energy Research (DIFFER), 5612 AJ Eindhoven, The Netherlands;* orcid.org/0000-0002-7154-1205; Email: r.sharma@differ.nl

Mihalis N. Tsampas − *Dutch Institute for Fundamental Energy Research (DIFFER), 5612 AJ Eindhoven, The Netherlands;* orcid.org/0000-0002-4367-4457; Phone: +31403334820; Email: m.tsampas@differ.nl

Authors

Hrishikesh Patel − *Dutch Institute for Fundamental Energy Research (DIFFER), 5612 AJ Eindhoven, The Netherlands*

Usman Mushtaq − *Dutch Institute for Fundamental Energy Research (DIFFER), 5612 AJ Eindhoven, The Netherlands*

Vasileios Kyriakou − *Dutch Institute for Fundamental Energy Research (DIFFER), 5612 AJ Eindhoven, The Netherlands*

Georgios Zafeiropoulos − *Dutch Institute for Fundamental Energy Research (DIFFER), 5612 AJ Eindhoven, The Netherlands*

Floran Peeters − *Dutch Institute for Fundamental Energy Research (DIFFER), 5612 AJ Eindhoven, The Netherlands*

Stefan Welzel − *Dutch Institute for Fundamental Energy Research (DIFFER), 5612 AJ Eindhoven, The Netherlands*

Mauritius C. M. van de Sanden − *Dutch Institute for Fundamental Energy Research (DIFFER), 5612 AJ Eindhoven, The Netherlands; Department of Applied Physics, Eindhoven University of Technology (TU.e), 5600 MB Eindhoven, The Netherlands;* orcid.org/0000-0002-4119-9971

Complete contact information is available at: https://pubs.acs.org/10.1021/acsenergylett.0c02349

Notes

The authors declare no competing financial interest.

https://dx.doi.org/10.1021/acsenergylett.0c02349
ACS Energy Lett. 2021, 6, 313−319

■ ACKNOWLEDGMENTS

This project has been cofinanced by TKI-Energie from Toeslag voor Topconsortia voor Kennis en Innovatie (TKI) from the Ministry of Economic Affairs and Climate Policy. The authors thank E. Langereis (DIFFER) and B. Lamers (DIFFER) for help with the illustrations and H. Dzafic (TU.e) for his contribution in completing the setup. ISPT, University of Twente, Nouryon, OCI Nitrogen, Vopak, and Yara are also acknowledged for their support in the project.

■ REFERENCES

(1) Good, A. Toward nitrogen-fixing plants. *Science* **2018**, *359*, 869−870.
(2) Wang, K.; Smith, D.; Zheng, Y. Electron-driven heterogeneous catalytic synthesis of ammonia: current states and perspective. *Carbon Resources Conversion* **2018**, *1* (1), 2−31.
(3) Fryzuk, M. D. Ammonia transformed. *Nature* **2004**, *427*, 498−499.
(4) Miura, D.; Tezuka, T. A comparative study of ammonia energy systems as a future energy carrier, with particular reference to vehicle use in Japan. *Energy* **2014**, *68*, 428−436.
(5) Demirci, U. B.; Miele, P. Sodium borohydride versus ammonia borane, in hydrogen storage and direct fuel cell applications. *Energy Environ. Sci.* **2009**, *2* (6), 627−637.
(6) Lan, R.; Irvine, J. T.; Tao, S. Ammonia and related chemicals as potential indirect hydrogen storage materials. *Int. J. Hydrogen Energy* **2012**, *37* (2), 1482−1494.
(7) Zamfirescu, C.; Dincer, I. Ammonia as a Green Fuel and Hydrogen Source for Vehicular Applications. *Fuel Process. Technol.* **2009**, *90*, 729−737.
(8) Maffei, N.; Pelletier, L.; Charland, J. P.; McFarlan, A. A direct ammonia fuel cell using barium cerate proton conducting electrolyte doped with gadolinium and praseodymium. *Fuel Cells* **2007**, *7* (4), 323−328.
(9) Davis, B. L.; Dixon, D. A.; Garner, E. B.; Gordon, J. C.; Matus, M. H.; Scott, B.; Stephens, F. H. Efficient regeneration of partially spent ammonia borane fuel. *Angew. Chem., Int. Ed.* **2009**, *48* (37), 6812−6816.
(10) Erisman, J. W.; Sutton, M. A.; Galloway, J.; Klimont, Z.; Winiwarter, W. How a century of ammonia synthesis changed the world. *Nat. Geosci.* **2008**, *1*, 636−639.
(11) Hargreaves, J. Nitrides as ammonia synthesis catalysts and as potential nitrogen transfer reagents. *Appl. Petrochem. Res.* **2014**, *4* (1), 3−10.
(12) Appl, M. *Ullmann's Encyclopedia of Industrial Chemistry*; Wiley, 2012; Vol. 3, pp 107−225.
(13) Schlogl, R. In *Handbook of Heterogeneous Catalysis*; Ertl, G.; Knözinger, H., Schüth, F., Weitkamp, J., Eds.; Wiley-VCH Verlag GmbH & Co. KGaA: Weinheim, 2008; pp 2501−2575.
(14) Smil, V. *Enriching the Earth: Fritz Haber, Carl Bosch, and the Transformation of World Food Production*; MIT Press, 2004; pp 1−358.
(15) Liu, H. Ammonia synthesis catalyst 100 years: practice, enlightenment and challenge. *Chin. J. Catal.* **2014**, *35*, 1619−1640.
(16) Gilland, B. Is a haber-bosch world Sustainable? Population, nutrition, cereals, nitrogen and environment. *J. Soc. Polit. Econ. Stud.* **2014**, *39* (2), 166−185.
(17) Vojvodic, A.; Medford, A. J.; Studt, F.; Abild-Pedersen, F.; Khan, T. S.; Bligaard, T.; Nørskov, J. K. Exploring the limits: a low-pressure, low-temperature Habere Bosch process. *Chem. Phys. Lett.* **2014**, *598*, 108−112.
(18) Gilbert, P.; Alexander, S.; Thornley, P.; Brammer, J. Assessing economically viable carbon reductions for the production of ammonia from biomass gasification. *J. Cleaner Prod.* **2014**, *64*, 581−589.
(19) Bardi, U.; El Asmar, T.; Lavacchi, A. Turning electricity into food: the role of renewable energy in the future of agriculture. *J. Cleaner Prod.* **2013**, *53*, 224−231.
(20) Bogaerts, A.; Neyts, E. C. Plasma Technology: An Emerging Technology for Energy Storage. *ACS Energy Lett.* **2018**, *3*, 1013−1027.
(21) Fridman, A. *Plasma Chemistry*; Cambridge University Press, 2008; pp 355−414.
(22) Utz, A. L. Vibrations that live long and prosper. *Nat. Chem.* **2018**, *10*, 577−578.
(23) Mehta, P.; Barboun, P.; Go, D. B.; Hicks, J. C.; Schneider, W. F. Catalysis Enabled by Plasma Activation of Strong Chemical Bonds: A Review. *ACS Energy Lett.* **2019**, *4* (5), 1115−1133.
(24) Patel, H.; Sharma, R. K.; Kyriakou, V.; Pandiyan, A.; Welzel, S.; van de Sanden, M. C. M.; Tsampas, M. N. *ACS Energy Letters* **2019**, *4* (9), 2091−2095.
(25) Neyts, E. C.; Ostrikov, K.; Sunkara, M. K.; Bogaerts, A. Plasma Catalysis: Synergistic Effects at the Nanoscale. *Chem. Rev.* **2015**, *115*, 13408−13446.
(26) Patil, B. S.; Van Kaathoven, A. S.; Peeters, F. J.; Cherkasov, N.; Lang, J.; Wang, Q.; Hessel, V. Deciphering the synergy between plasma and catalyst support for ammonia synthesis in a packed dielectric barrier discharge reactor. *J. Phys. D: Appl. Phys.* **2020**, *53* (14), 144003.
(27) Gomez-Ramirez, A.; Cotrino, J.; Lambert, R.; Gonzalez-Elipe, A. Efficient Synthesis of Ammonia from N_2 and H_2 Alone in a Ferroelectric Packed-bed DBD Reactor. *Plasma Sources Sci. Technol.* **2015**, *24*, 065011.
(28) Aihara, K.; Akiyama, M.; Deguchi, T.; Tanaka, M.; Hagiwara, R.; Iwamoto, M. Remarkable Catalysis of a Wool-like Copper Electrode for NH_3 Synthesis from N_2 and H_2 in Non-Thermal Atmospheric Plasma. *Chem. Commun.* **2016**, *52*, 13560−13563.
(29) Akay, G.; Zhang, K. Process Intensification in Ammonia Synthesis Using Novel Co assembled Supported Microporous Catalysts Promoted by Nonthermal Plasma. *Ind. Eng. Chem. Res.* **2017**, *56*, 457−468.
(30) Peng, P.; Chen, P.; Schiappacasse, C.; Zhou, N.; Anderson, E.; Chen, D.; Liu, J.; Cheng, Y.; Hatzenbeller, R.; Addy, M.; Zhang, Y. A review on the non-thermal plasma-assisted ammonia synthesis Technologies. *J. Cleaner Prod.* **2018**, *177*, 597−609.
(31) Harada, K.; Igari, S.; Takasaki, M.; Shimoyama, A. Reductive fixation of molecular nitrogen by glow discharge against water. *J. Chem. Soc., Chem. Commun.* **1986**, *17*, 1384−1385.
(32) Bian, W.; Shi, J.; Yin, X. Nitrogen fixation into water by pulsed high-voltage discharge. *IEEE Trans. Plasma Sci.* **2009**, *37* (1), 211−218.
(33) Gorbanev, Y.; Vervloessem, E.; Nikiforov, A.; Bogaerts, A. Nitrogen Fixation with Water Vapor by Nonequilibrium Plasma: toward Sustainable Ammonia Production. *ACS Sustainable Chem. Eng.* **2020**, *8* (7), 2996−3004.
(34) Toth, J. R.; Abuyazid, N. H.; Lacks, D. J.; Renner, J. N.; Sankaran, R. M. A plasma-water droplet reactor for process-intensified, continuous nitrogen fixation at atmospheric pressure. *ACS Sustainable Chem. Eng.* **2020**, *8* (39), 14845−14854.
(35) Matsumoto, O. Plasma Catalytic Reaction in Ammonia Synthesis in the Microwave Discharge. *J. Phys. IV* **1998**, *8*, 7−411.
(36) Uyama, H.; Nakamura, T.; Tanaka, S.; Matsumoto, O. Catalytic Effect of Iron Wires on the Syntheses of Ammonia and Hydrazine in a Radio-Frequency Discharge. *Plasma Chem. Plasma Process.* **1993**, *13*, 117−131.
(37) Shah, J.; Wang, W.; Bogaerts, A.; Carreon, M. L. Ammonia synthesis by radio frequency plasma catalysis: revealing the underlying mechanisms. *ACS Applied Energy Materials* **2018**, *1* (9), 4824−4839.
(38) Shah, J.; Wu, Ting; Lucero, J.; Carreon, M. A.; Carreon, M. L. Nonthermal Plasma Synthesis of Ammonia over Ni-MOF-74, ACS Sustainable. *ACS Sustainable Chem. Eng.* **2019**, *7* (1), 377−383.
(39) Van Helden, J.; Wagemans, W.; Yagci, G.; Zijlmans, R.; Schram, D.; Engeln, R.; Lombardi, G.; Stancu, G.; Röpcke, J. Detailed Study of the Plasma-Activated Catalytic Generation of Ammonia in N_2-H_2 Plasmas. *J. Appl. Phys.* **2007**, *101*, 043305−043316.
(40) Carrasco, E.; Jiménez-Redondo, M.; Tanarro, I.; Herrero, V. J. Neutral and ion chemistry in low pressure dc plasmas of H_2/N_2 mixtures: routes for the efficient production of NH_3 and NH_4^+. *Phys. Chem. Chem. Phys.* **2011**, *13* (43), 19561−19572.

(41) Gorse, C.; Cacciatore, M.; Capitelli, M.; De Benedictis, S.; Dilecce, G. Electron energy distribution functions under N_2 discharge and post-discharge conditions: a self-consistent approach. *Chem. Phys.* **1988**, *119*, 63−70.
(42) Ricard, A.; Sarrette, J. P.; Jeon, B.; Kim, Y. K. Discharge source dependent variation in the densities of active species in the flowing afterglows of N_2 RF and UHF plasmas. *Curr. Appl. Phys.* **2017**, *17*, 945−950.
(43) Guerra, V.; Galiaskarov, E.; Loureiro, J. Dissociation mechanisms in nitrogen discharges. *Chem. Phys. Lett.* **2003**, *371* (5−6), 576−581.
(44) Gatti, N.; Ponduri, S.; Peeters, F. J. J.; Van Den Bekerom, D. C. M.; Minea, T.; Tosi, P.; van de Sanden, M. C. M.; Van Rooij, G. J. Preferential vibrational excitation in microwave nitrogen plasma assessed by Raman scattering. *Plasma Sources Sci. Technol.* **2018**, *27* (5), 055006−055028.
(45) Mehta, P.; Barboun, P.; Herrera, F. A.; Kim, J.; Rumbach, P.; Go, D. B.; Hicks, J. C.; Schneider, W. F. Overcoming ammonia synthesis scaling relations with plasma-enabled catalysis. *Nat. Catal.* **2018**, *1*, 269−275.
(46) Barboun, P.; Mehta, P.; Herrera, F. A.; Go, D. B.; Schneider, W. F.; Hicks, J. C. Distinguishing Plasma Contributions to Catalyst Performance in Plasma-Assisted Ammonia Synthesis. *ACS Sustainable Chem. Eng.* **2019**, *7* (9), 8621−8630.
(47) Giddey, S.; Badwal, S. P. S.; Kulkarni, A. Review of electrochemical ammonia production technologies and materials. *Int. J. Hydrogen Energy* **2013**, *38*, 14576−14594.
(48) Amar, I. A.; Lan, R.; Petit, C. T.; Tao, S. W. Solid-state electrochemical synthesis of ammonia: a review. *J. Solid State Electrochem.* **2011**, *15*, 1845−1860.
(49) Kyriakou, V.; Garagounis, I.; Vasileiou, E.; Vourros, A.; Stoukides, M. Progress in the Electrochemical Synthesis of Ammonia. *Catal. Today* **2017**, *286*, 2−13.
(50) Ohrelius, M.; Guo, H.; Xian, H.; Yu, G.; Alshehri, A. A.; Alzahrani, K. A.; Li, T.; Andersson, M. Electrochemical Synthesis of Ammonia Based on a Perovskite $LaCrO_3$ Catalyst. *ChemCatChem* **2020**, *12*, 731−735.
(51) Soloveichik, G. Electrochemical synthesis of ammonia as a potential alternative to the Haber−Bosch process. *Nature Catalysis* **2019**, *2* (5), 377−380.
(52) Kyriakou, V.; Garagounis, I.; Vourros, A.; Vasileiou, E.; Stoukides, M. An Electrochemical Haber-Bosch Process. *Joule* **2020**, *4*, 142.
(53) Amar, I. A.; Petit, C. T.; Mann, G.; Lan, R.; Skabara, P. J.; Tao, S. Electrochemical synthesis of ammonia from N_2 and H_2O based on (Li, Na, K)$_2CO_3$−$Ce_{0.8}Gd_{0.18}Ca_{0.02}O_{2-\delta}$ composite electrolyte and $CoFe_2O_4$ cathode. *Int. J. Hydrogen Energy* **2014**, *39*, 4322−4330.
(54) Lan, R.; Alkhazmi, K. A.; Amar, I. A.; Tao, S. Synthesis of ammonia directly from wet air using new perovskite oxide $La_{0.8}Cs_{0.2}Fe_{0.8}Ni_{0.2}O_{3-\delta}$ as catalyst. *Electrochim. Acta* **2014**, *123*, 582−587.
(55) Hao, Y. C.; Guo, Y.; Chen, L. W.; Shu, M.; Wang, X. Y.; Bu, T. A.; Gao, W. Y.; Zhang, N.; Su, X.; Feng, X.; Zhou, J. W. Promoting nitrogen electroreduction to ammonia with bismuth nanocrystals and potassium cations in water. *Nature Catalysis* **2019**, *2* (5), 448−456.
(56) Zhou, F. L.; Azofra, L. M.; Ali, M.; Kar, M.; Simonov, A. N.; McDonnell-Worth, C.; Sun, C.; Zhang, Z.; R. MacFarlane, D. R. Electro-synthesis of ammonia from nitrogen at ambient temperature and pressure in ionic liquids. *Energy Environ. Sci.* **2017**, *10*, 2516−2520.
(57) Marnellos, G.; Stoukides, M. Ammonia synthesis at atmospheric pressure. *Science* **1998**, *282*, 98−100.
(58) Hawtof, R.; Ghosh, S.; Guarr, E.; Xu, C.; Sankaran, R. M.; Renner, J. N. Catalyst-free, highly selective synthesis of ammonia from nitrogen and water by a plasma electrolytic system. *Sci. Adv.* **2019**, *5*, 5778−5788.
(59) Kumari, S.; Pishgar, S.; Schwarting, M. E.; Paxton, W. F.; Spurgeon, J. M. Synergistic plasma-assisted electrochemical reduction of nitrogen to ammonia. *Chem. Commun.* **2018**, *54* (95), 13347−13350.
(60) Skulason, E.; Bligaard, T.; Gudmundsdottir, S.; Studt, F.; Rossmeisl, J.; Abild-Pedersen, F.; Vegge, T.; Jónsson, H.; Nørskov, J. K. A theoretical evaluation of possible transition metal electro-catalysts for N_2 reduction. *Phys. Chem. Chem. Phys.* **2012**, *14*, 1235−1245.
(61) Vernoux, P.; Lizarraga, L.; Tsampas, M. N.; Sapountzi, F. M.; De Lucas-Consuegra, A.; Valverde, J. L.; Souentie, S.; Vayenas, C. G.; Tsiplakides, D.; Balomenou, S.; Baranova, E. Ionically conducting ceramics as active catalytic supports. *Chem. Rev.* **2013**, *113* (10), 8192−8260.
(62) Łukaszewski, M.; Soszko, M.; Czerwinski, A. Electrochemical methods of real surface area determination of noble metal electrodes−an overview. *Int. J. Electrochem. Sci.* **2016**, *11*, 4442−4469.
(63) Ogura, Y.; Sato, K.; Miyahara, S. I.; Kawano, Y.; Toriyama, T.; Yamamoto, T.; Matsumura, S.; Hosokawa, S.; Nagaoka, K. Efficient ammonia synthesis over a $Ru/La_{0.5}Ce_{0.5}O_{1.75}$ catalyst pre-reduced at high temperature. *Chemical science* **2018**, *9* (8), 2230−2237.
(64) Guerra, V.; Sá, P. A.; Loureiro, J. Electron and metastable kinetics in the nitrogen afterglow. *Plasma Sources Sci. Technol.* **2003**, *12* (4), S8−S15.
(65) Amorim, J.; Baravia, G.; Ricard, A. Production of N, H, and NH active species in N_2-H_2 dc flowing discharges. *Plasma Chem. Plasma Process.* **1995**, *15* (4), 721−731.
(66) Gordiets, B.; Ferreira, C. M.; Pinheiro, M. J.; Ricard, A. Self-consistent kinetic model of low-pressure N2−H2 flowing discharges: I. Volume processes. *Plasma Sources Sci. Technol.* **1998**, *7*, 363−378.
(67) Lazouski, N.; Chung, M.; Williams, K.; Gala, M. L.; Manthiram, K. Non-aqueous gas diffusion electrodes for rapid ammonia synthesis from nitrogen and water-splitting-derived hydrogen. *Nature Catalysis* **2020**, *3* (5), 463−469.
(68) McEnaney, J. M.; Singh, A. R.; Schwalbe, J. A.; Kibsgaard, J.; Lin, J. C.; Cargnello, M.; Jaramillo, T. F.; Nørskov, J. K. Ammonia synthesis from N_2 and H_2O using a lithium cycling electrification strategy at atmospheric pressure. *Energy Environ. Sci.* **2017**, *10* (7), 1621−1630.
(69) Papaioannou, E. I.; Bachmann, C.; Neumeier, J. J.; Frankel, D.; Over, H.; Janek, J.; Metcalfe, I. A. Role of the Three-Phase Boundary of the Platinum−Support Interface in Catalysis: A Model Catalyst Kinetic Study. *ACS Catal.* **2016**, *6* (9), 5865−5872.

https://dx.doi.org/10.1021/acsenergylett.0c02349
ACS Energy Lett. 2021, 6, 313−319